



DESIGN ASPECTS OF SOLAR THERMOCHEMICAL ENGINEERING—A CASE STUDY: TWO-STEP WATER-SPLITTING CYCLE USING THE Fe₃O₄/FeO REDOX SYSTEM

A. STEINFELD*[†], S. SANDERS** and R. PALUMBO*

*High-temperature Solar Technology, Paul Scherrer Institute, 5132 Villigen-PSI, Switzerland

**Valparaiso University, Valparaiso, IN 46383, U.S.A.

Revised version accepted 17 July 1998

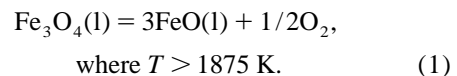
Abstract—We describe a methodology for the initial development of solar thermochemical reactors for converting concentrated solar energy into chemical fuels. It consists of determining the implications that the thermodynamics and kinetics of the chemical transformation have on the initial reactor design. The method is applied for a specific case study: the decomposition of iron oxide above 1875 K, as part of a two-step thermochemical cycle for producing hydrogen from water. We demonstrate that the chemistry of the reaction places important constraints on various engineering design aspects, and we present two reactor concepts that satisfy these constraints. This study addresses the initial steps necessary for the design and development of solar chemical reactors. © 1998 Elsevier Science Ltd. All rights reserved.

1. INTRODUCTION

Although work in the area of high-temperature solar chemistry started at least as far back as 1952 with the work of Dr. Trombe in Mont Lois France (Lede and Pharabod, 1997), a scientific discipline known as high-temperature solar chemistry has not yet emerged from the research; solar chemistry is not a field of study at any university in the world. This fact is not surprising given the very small world-wide financial commitment to the research. Nonetheless, a number of scientists and engineers since 1952 have been looking at how the energy in the form of sunlight in the sunbelt regions of the world can be transported as chemical energy to population centers. No text book exists that demonstrates the techniques for designing the solar chemical plant. Rather, the methodology for such a task is being created as the research advances.

At this juncture in time, the methods for selecting chemical reactions for storing sunlight, the methodology for studying these reactions, and the techniques for developing the technology for effecting the chemical reactions are all germane subjects for discussion. In this paper, we would like to focus on what we have found to be some of the main issues associated with the develop-

ment of a solar reactor concept for a given chemical reaction. We present our ideas in the form of a case study. Specifically, we demonstrate how we arrived at reactor concepts for effecting the following chemical transformation:



This reaction is at the heart of two major ideas for storing sunlight in the form of chemical energy. FeO reacts exothermally at low temperature with either H₂O or CO₂ to produce H₂ or C(gr) according to Eqs. (2) and (3) respectively.



The Fe₃O₄ that is produced in either of these two reactions is recycled to a solar furnace where FeO is reproduced from the reaction [Eq. (1)]. In this manner, solar energy is used to produce either H₂ from H₂O or C(gr) from CO₂ (Nakamura, 1977; Ehrensberger *et al.*, 1997). The two-step water-splitting cycle represented by the reactions [Eq. (1)][Eq. (2)] is schematically shown in Fig. 1.

2. GENERAL CONSTRAINTS FOR THE DESIGN PROBLEM

Because a long term goal of the research is to have solar energy become the significant sustainable energy resource for the world economy, it is

[†]Author to whom correspondence should be addressed. Tel.: +41-56-310-3124; fax: +41-56-310-3160; e-mail: aldo.steinfeld@psi.ch

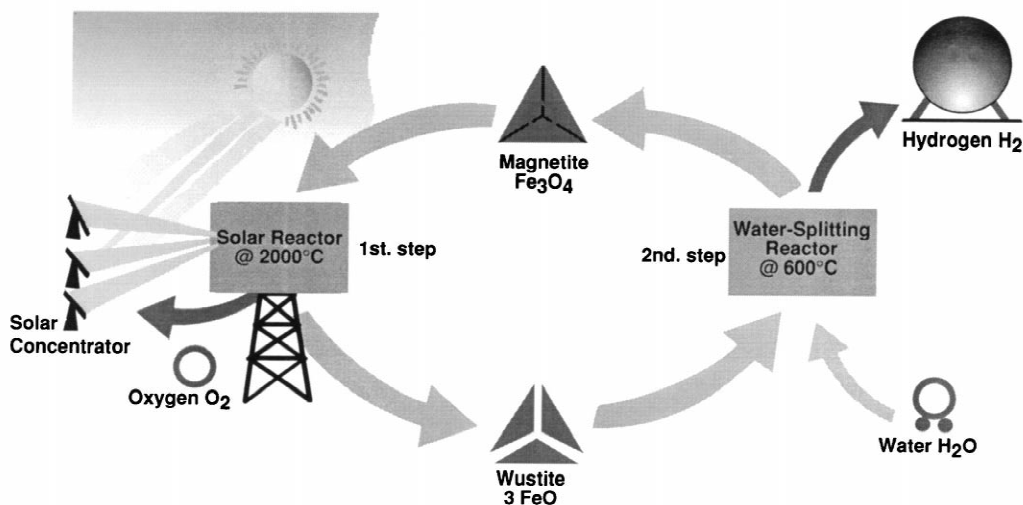


Fig. 1. Schematic representation of a two-step water-splitting solar thermochemical cycle using the $\text{Fe}_3\text{O}_4/\text{FeO}$ redox system. In the first, endothermic, solar step, magnetite (Fe_3O_4) is thermally decomposed into wustite (FeO) and oxygen at elevated temperatures. Concentrated solar energy is the source of high-temperature process heat. In the second, exothermic step, wustite is reacted with water to form hydrogen; magnetite is recycled to the first step. The net reaction is: $\text{H}_2\text{O} = \text{H}_2 + 0.5\text{O}_2$; hydrogen and oxygen are produced in different steps, eliminating the need for high-temperature gas separation.

important that the development of the solar chemical reactor be shaped by economic considerations. It is pertinent to ask how one can be concerned with the economics of a technology that does not exist especially when its use is envisioned for a time at least 50 years into the future. Certainly a typical cost benefit analysis is inappropriate; if such a criteria were invoked in the 19th and early 20th century by potential entrepreneurs, it seems likely that they would have decided not to invent the telephone, oil refinery, automobile, aircraft, etc. In place of a cost benefit analysis, we consider very general economic constraints on the design problem. This approach means that we identify aspects of the technology that are likely to be costly and then attempt to make design decisions that favor the least expensive options relative to the choices at hand.

To date, the largest single cost element of a solar central receiver power plant is the heliostat field and it typically represents between 30 and 40% of the total capital cost (De Laquil, 1994). Thus, economics suggests at one level that the solar chemical reactor effect the chemical transformation with the highest possible thermal efficiency so that the size of the heliostat field can be kept to a minimum. The cost of the reactor, however, can go up as one attempts to maximize its thermal efficiency. For example, a reactor closed by a transparent window may be more efficient than one open to the atmosphere, but its

cost could be significantly higher with the window, both from initial investment and daily maintenance points of view. Heat exchanger equipment may substantially boost thermal efficiency by adding pre-heating to the process, but it comes with a price. Thus, it is important to accurately estimate the gain in thermal efficiency for a given design decision as well as to develop alternate reactor concepts that can be followed as time elucidates the best economic path to follow.

We demonstrate that the chemistry of the reaction conducted in the solar chemical reactor plays a vital role in determining the reactor's thermal efficiency. We begin, by presenting the chemical thermodynamics and kinetics for reaction [Eq. (1)].

3. THE CHEMISTRY FOR Fe_3O_4 DECOMPOSITION AND ITS IMPLICATIONS ON REACTOR DESIGN

3.1. Chemical thermodynamics

We expect the gas phase products in air to be O , O_2 , N_2 , NO , and $\text{FeO}(\text{g})$. The liquid phase will be a mixture of $\text{FeO}(\text{l})$ and $\text{Fe}_3\text{O}_4(\text{l})$. Since the activity coefficients for a mixture of these two liquids are not known, equilibrium calculations were performed assuming either an immiscible mixture or an ideal solution of $\text{FeO}(\text{l})$ and $\text{Fe}_3\text{O}_4(\text{l})$.

Chemical equilibrium compositions were com-

puted using the STANJAN computer code (Reynolds, 1986). Thermochemical data was taken from JANAF Thermochemical Tables (1985). The reactants are 1 mole $\text{Fe}_3\text{O}_4(\text{s})$ and x moles of air, where x depends on the loading ratio of iron oxide in air. The results are shown in Table 1. Species with mole fractions less than 10^{-5} have been omitted. The conversion ratio is defined as the number of FeO moles in equilibrium (in any phase) divided by 3 (which corresponds to the complete conversion of 1 mole of Fe_3O_4 to 3 moles of FeO and 0.5 moles of O_2). Case 0 is the only case where we presume the condensed phase to be an immiscible mixture and obtain 100% conversion ratio. All the other cases assume the chemical equilibrium composition for an ideal solution. Computations were made for three different air/ Fe_3O_4 molar ratios (0, 1, and 10) and for four different reactor temperatures (1900 K, 2100 K, 2300 K, and 2500 K). The different cases are grouped as Case 1, 2, and 3 for air/ Fe_3O_4 molar ratios 0, 1, and 10, respectively; and are further grouped in Case 1_{-1} , 2_{-3} , and 4_{-4} for temperatures 1900, 2100, 2300, and 2500 K, respectively.

For all cases, the conversion increases with temperature and with air/ Fe_3O_4 molar ratio, ranging from 11% for Case 1_{-1} (lowest temperature and air/ Fe_3O_4 molar ratio) to 52% for Case

3_{-4} (highest temperature and air/ Fe_3O_4 molar ratio). As the temperature increases, FeO(l) becomes the major component in the condensed phase. For example, for Cases 2_{-1} to 2_{-4} , the mole percent of FeO in the liquid phase for an equilibrium system goes from 33% to 73% when the temperature varies between 1900 K and 2500 K. There is little FeO(g) present in the gas phase and we must presume that it will re-oxidize to Fe_3O_4 and Fe_2O_3 , as evidenced by solar experimentation (Tofighi and Sibieude, 1980; Sibieude *et al.*, 1982; Tofighi and Sibieude, 1984).

If the number of moles of air is markedly increased, slightly more FeO(l) is produced at each temperature, but substantially more FeO(g) is also produced. Thus, for an atmospheric-open reactor, it will be necessary to continuously remove the liquid phase, if the forming of FeO(g) is to be avoided. When no air is present in the system (Cases 1_{-1} to 1_{-4}), the mole percent of FeO in the liquid phase goes from 27% to 67% between 1900 and 2500 K. At 2500 K, FeO(g) starts to become significant. This result is important too – under air, more FeO is obtained than in the case of no air, but a portion of the delivered solar energy is used to heat the air. An additional drawback when effecting the reaction in air is the formation of NO_x compounds. However, a techni-

Table 1. Molar composition of the products at the exit of the solar reactor and energy balance on the two-step water-splitting cycle scheme

Case	0	1_{-1}	1_{-2}	1_{-3}	1_{-4}	2_{-1}	2_{-2}	2_{-3}	2_{-4}	3_{-1}	3_{-2}	3_{-3}	3_{-4}
x , air/ Fe_3O_4 molar ratio	0	0				1				10			
T_{reactor} (K)	2300	1900	2100	2300	2500	1900	2100	2300	2500	1900	2100	2300	2500
Product composition	-	Chemical thermodynamic equilibrium											
$\text{Fe}_3\text{O}_4(\text{l})$	0	0.8890	0.8160	0.7180	0.5960	0.8579	0.7680	0.6510	0.5148	0.8527	0.7549	0.6253	0.4741
FeO(l)	3	0.3330	0.5510	0.8460	1.2101	0.4262	0.6960	1.0470	1.4500	0.4420	0.7352	1.1230	1.5700
FeO(g)	0	<1e-5	<1e-5	<1e-5	1.05e-4	<1e-5	<1e-5	<1e-5	<1e-5	<1e-5	<1e-5	7.86e-4	6.14e-3
O_2	0.5	5.55e-2	0.0918	0.1410	0.2003	0.2770	0.3192	0.3720	0.4300	2.142	2.166	2.191	2.206
N_2	0	<1e-5	<1e-5	<1e-5	<1e-5	0.7860	0.7835	0.7790	0.7730	7.8690	7.8470	7.8160	7.7770
NO	0	<1e-5	<1e-5	<1e-5	<1e-5	6.93e-3	0.0129	0.0219	0.0342	0.0609	0.1068	0.1682	0.2406
O	0	1.64e-5	1.27e-4	6.95e-4	2.90e-3	1.60e-4	8.33e-4	3.26e-3	0.0105	1.38e-3	6.46e-3	2.33e-2	6.85e-2
Conversion ratio (%)	100%	11.1%	18.4%	28.2%	40.3%	14.2%	23.2%	34.9%	48.3%	14.7%	24.5%	37.4%	52.3%
Energy balance													
Q_{solar} (kW)	1148.6	578.3	708.8	905.8	1240.2	649.6	802.2	1031.7	1418.7	1218.3	1516.3	1960.9	2714.9
Q_{rerad} (kW)	364.6	85.5	156.3	287.5	549.4	96.0	176.9	327.4	628.5	180.1	334.4	622.3	1202.7
$Q_{\text{reactor,net}}$ (kW)	784.0	492.8	552.4	618.3	690.8	553.6	625.3	704.3	790.2	1038.2	1181.8	1338.5	1512.2
Q_{quench} (kW)	478.3	458.9	496.3	532.2	567.5	510.3	554.4	597.7	642.1	993.4	1107.1	1224.2	1350.7
Q_{ws} (kW)	18.0	2.0	3.3	5.1	7.3	2.6	4.2	6.3	8.7	2.7	4.4	6.7	9.4
Q_{FC} (kW)	53.8	6.0	9.9	15.2	21.7	7.6	12.5	18.8	26.0	7.9	13.2	20.1	28.2
$\eta_{\text{absorption}}$ (%)	68.3%	85.2%	77.9%	68.3%	55.7%	85.2%	77.9%	68.3%	55.7%	85.2%	77.9%	68.3%	55.7%
W_{FC} (kW)	233.9	26.0	43.0	66.0	94.4	33.2	54.3	81.7	113.1	34.5	57.3	87.6	122.4
$I_{\text{rr,quench}}/Q_{\text{solar}}$ (K^{-1})	1.02e-3	1.91e-3	1.71e-3	1.45e-3	1.15e-3	1.88e-3	1.68e-3	1.43e-3	1.13e-3	1.89e-3	1.73e-3	1.51e-3	1.23e-3
η_{overall} (%)	20.4%	4.5%	6.1%	7.3%	7.6%	5.1%	6.8%	7.9%	7.9%	2.8%	3.8%	4.5%	4.5%
$\eta_{\text{overall,max}}$ (%)	50.7%	61.3%	57.0%	50.6%	41.8%	61.0%	56.7%	50.4%	41.7%	59.2%	55.4%	49.6%	41.2%

Species with mole fractions less than 10^{-5} have been omitted. The baseline configuration is used unless otherwise stated. Mass flow-rate of reactants is $1 \text{ mol s}^{-1} \text{ Fe}_3\text{O}_4 + x \text{ mol s}^{-1} \text{ air}$.

cal advantage is that an open reactor eliminates the need for a transparent window at the reactor aperture. The added complexity of a window must be evaluated along with any potential thermodynamic gains.

3.2. Chemical kinetics

The available rate expression for the decomposition of liquid Fe_3O_4 is described by Tofighi (1982):

$$d\xi/dt = k\xi^{0.5}(1 - \xi)^{0.77} \quad (4)$$

where ξ is the degree of reaction varying between 0 and 1, as measured by the amount of O_2 that is produced, and k is the rate constant: $k = 2.66 \exp(-1250/T) \text{ min}^{-1}$. This expression was shown to have limited applicability because it does not account for the partial pressure of oxygen: although the kinetic experiments from which the above rate expression was established were conducted under a 20 l h^{-1} flow of Ar, it was shown that as the Ar flow-rate increased, the rate increased (Tofighi, 1982). Nonetheless, several conclusions can be drawn from the study. Under Ar flowing at 20 l h^{-1} , and a temperature of 2100 K, the decomposition rate reaches a maximum value near 40% completion (Tofighi, 1982). The rate of decomposition is being limited by the gas phase mass transport of O_2 from the liquid surface. We expect the reaction in air to be slower than that predicted by Eq. (4).

It is important to note that partial substitution of iron in Fe_3O_4 by metals M such as Mn, Mg, and Co, forms mixed metal oxides $(\text{Fe}_{1-x}\text{M}_x)_3\text{O}_4$ that may be reducible at lower temperatures than those required for the reduction of Fe_3O_4 , while the reduced phase $(\text{Fe}_{1-x}\text{M}_x)_{1-y}\text{O}$ is still capable of splitting water (Kuhn *et al.*, 1995; Tamaura *et al.*, 1995). Reduction yields between 4% to 37% were obtained using a suspension of $4\text{-}\mu\text{m}$ particles in N_2 that were exposed for short times (less than 1 s) to solar flux intensities of 5000 kW m^{-2} (Steiner, 1997). Under similar conditions, but using air instead as the carrier gas, the products revealed no reduction but rather further oxidation. Thus, although such a chemical system would require a moderate (and more workable) upper operating temperature for the reduction, the experimental results with particle suspensions suggest the need to provide either fast quenching or an oxygen-free atmosphere to avoid re-oxidation. Segregation effects, due to different affinities to oxygen and different diffusion coefficients, were observed during the thermal reduction in N_2 atmosphere that lasted 10 s (Nüesch, 1996); no

such effects were found in faster solar experiments with residence times of less than 1 s. Segregation, unless reversible, would severely hinder the recycling capability of mixed metal oxides redox systems. Laboratory experiments on the water-splitting reaction have shown that the rate of reaction is slower; the reaction time to 50% completion is about twice as long when using the reduced form of Fe–Mn mixed oxides than when using wustite (Ehrensberger *et al.*, 1995). For each of these reasons, we prefer Fe_3O_4 as the starting material.

To see all of the consequences of the decomposition kinetics on the design of a reactor would require solving for various reactor concepts, the energy and mass balance equations simultaneously with a valid expression given for the rate of the reaction. This numerical task is beyond the scope of this study. Nevertheless, a look at the rate expression gives some insights on the reactor design. Because the reaction rate peaks at a given conversion, the reactor should not be operated beyond the condition where the rate is a maximum. Such a design constraint attempts to maximize the production rate of FeO.

It has been demonstrated that the back reaction between FeO(l) and O_2 is very fast (Tofighi, 1982). Quenching the decomposition products at a rate of $10\,000 \text{ K s}^{-1}$ was necessary to obtain good FeO yields. It will be shown in the following section that this fact places severe constraints on the reactor designer attempting to maximize the thermal efficiency of a solar process using the Fe_3O_4 decomposition step.

4. THE THERMODYNAMIC CYCLE ANALYSIS AND ITS IMPLICATIONS ON REACTOR DESIGN

This section presents a second-law analysis that assesses the maximum possible efficiency of a two-step water-splitting solar thermochemical cycle using the $\text{Fe}_3\text{O}_4/\text{FeO}$ redox system. This cycle, represented by Eqs. (1) and (2), has been previously analyzed (Nakamura, 1977), but this previous study did not account for the solar energy absorption efficiency and did not consider equilibrium compositions nor the effect of heating and quenching air. The present second-law analysis accounts for these important constraints and follows the derivation of Steinfeld *et al.* (1996).

A quasi-cyclic system that allows for energy and mass to cross the boundaries is considered. The process flow sheet is shown in Fig. 2. It is an archetypal model which uses a solar reactor, a quenching device, a water-splitter reactor, and a

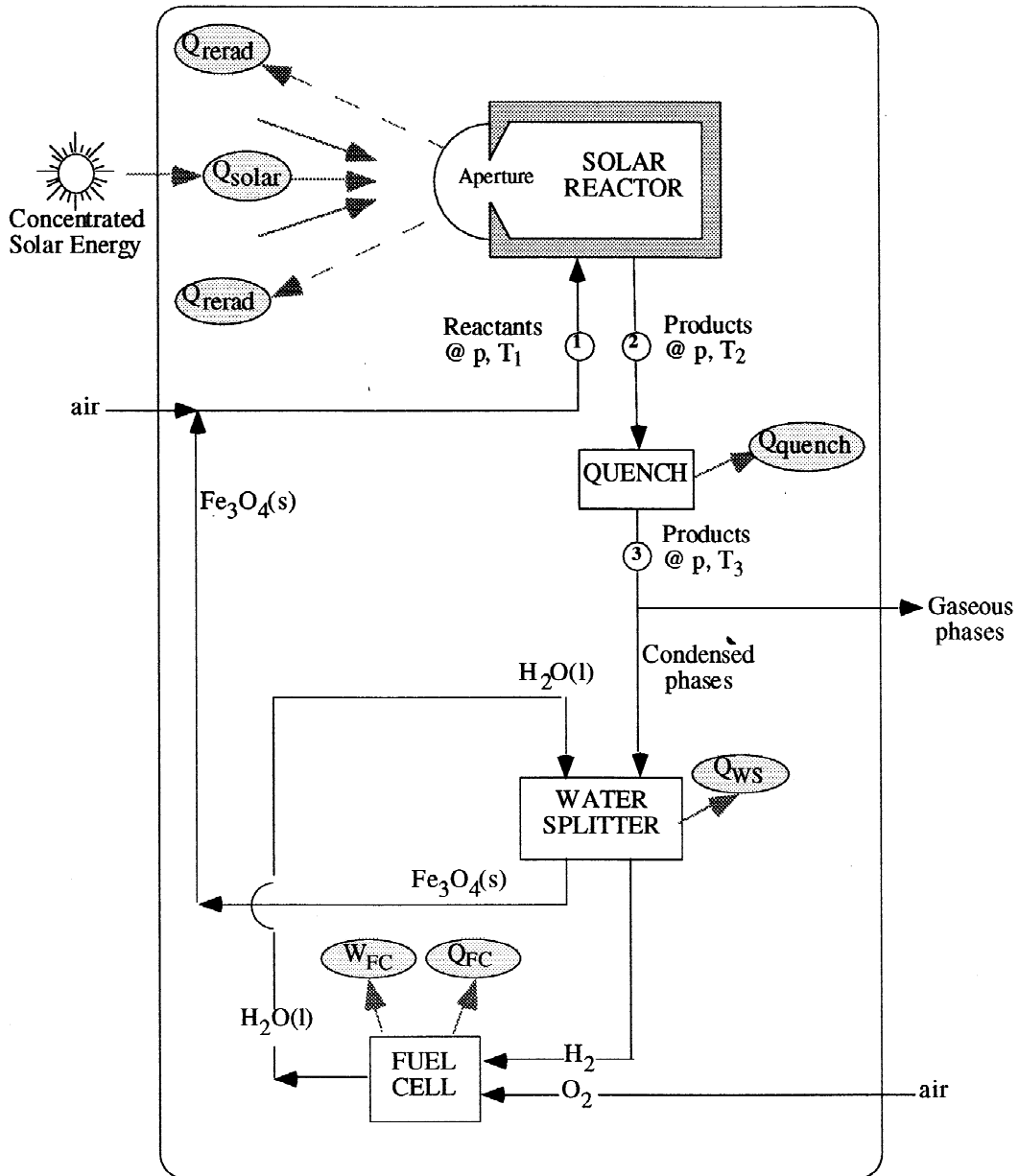


Fig. 2. The process flow diagram modelling the two-step water-splitting thermochemical cycle using $\text{Fe}_3\text{O}_4/\text{FeO}$ and solar energy. It is an archetypal model which uses a solar reactor, a quenching device, a water-splitter reactor, and a fuel cell. A mixture of 1 mol s^{-1} of $\text{Fe}_3\text{O}_4(\text{s})$ and $x \text{ mol s}^{-1}$ of air is fed into the process at $T_1 = 298 \text{ K}$ and a pressure of 1 bar.

fuel cell. A mixture of 1 mol s^{-1} of $\text{Fe}_3\text{O}_4(\text{s})$ and $x \text{ mol s}^{-1}$ of air is fed into the process at $T_1 = 298 \text{ K}$ and a pressure of 1 bar. The complete process is carried out at constant pressure. In practice, pressure drops will occur throughout the system. If one assumes, however, frictionless operating conditions, no pumping work is required.

4.1. Solar Reactor

The solar reactor is assumed to be a cavity-receiver having a small aperture to let in concentrated solar radiation. Its solar energy absorption efficiency, $\eta_{\text{absorption}}$, is defined as the net rate at

which energy is being absorbed divided by the solar power coming from the concentrator. For a perfectly insulated blackbody cavity receiver (no convection or conduction heat losses; only radiation losses through the aperture are considered; $\alpha_{\text{eff}} = \epsilon_{\text{eff}} = 1$), it is given by (Fletcher and Moen, 1977):

$$\eta_{\text{absorption}} = \frac{Q_{\text{reactor,net}}}{Q_{\text{solar}}} = 1 - (\sigma T_{\text{reactor}}^4 / I\tilde{C}) \quad (5)$$

The reactants enter the solar reactor at T_1 and are further heated to the reactor temperature T_{reactor} .

Chemical equilibrium is assumed inside the reactor. Thus, the reactants undergo a chemical transformation as they are heated to T_{reactor} . Q_{solar} is the total power coming from the solar concentrator. Q_{rerad} is the power lost by reradiation through the reactor aperture. Radiation gain from the environment is ignored. The net power absorbed in the solar reactor should match the enthalpy change of the reaction, i.e.:

$$Q_{\text{reactor,net}} = \Delta H|_{\text{Reactants}@T_{1,p} \rightarrow \text{Products}@T_{2,p}}. \quad (6)$$

Products exit the solar reactor at $T_2 = T_{\text{reactor}}$, having an equilibrium composition.

4.2. Quench

After leaving the reactor, the products are cooled rapidly to ambient temperature, $T_3 = 298$ K. The product composition remains unchanged as they are quenched, except for the phase changes (e.g., FeO(l) to FeO(s); Fe₃O₄(l) to Fe₃O₄(s)) and the reformation of O₂ and N₂ from O and NO. This assumption is reasonable provided the kinetics of the reoxidation of FeO is slower than the time it takes to quench. The amount of thermal power lost during quenching is:

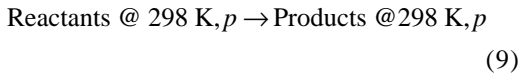
$$Q_{\text{quench}} = -\Delta H|_{\text{Products}@T_{2,p} \rightarrow \text{Products}@T_{3,p}}. \quad (7)$$

The irreversibility associated with quenching is:

$$Irr_{\text{quench}} = (Q_{\text{quench}}/298) + (\Delta S|_{\text{Products}@T_{2,p} \rightarrow \text{Products}@T_{3,p}}). \quad (8)$$

Quenching is a completely irreversible step causing a significant drop in the system efficiency.

From point 1 to 3 in the flow sheet, the chemical transformation:



has been effected. The products separate naturally into gaseous and condensed phases without expending work; gases are discarded to the atmosphere.

4.3. Water-Splitter

FeO reacts exothermally with water to form molecular H₂ according to Eq. (2), which takes place in the water-splitter reactor of Fig. 2. The heat liberated could be used in an auto-thermal reactor for conducting the water-splitting reaction at temperatures above ambient conditions. In this study, however, we consider this heat lost to the surroundings, as given by:

$$Q_{\text{WS}} = -\Delta H|_{3\text{FeO(s)} + \text{H}_2\text{O(l)} \rightarrow \text{Fe}_3\text{O}_4\text{(s)} + \text{H}_2}. \quad (10)$$

4.4. Fuel Cell

The hydrogen produced in the water-splitter reactor may be burned in air and the heat of combustion converted into work via a heat engine, or it may be used more efficiently in a fuel cell to generate electric work directly. The theoretical maximum available work that could be extracted from hydrogen is calculated by introducing a reversible fuel cell, represented in Fig. 2 as FUEL CELL. In this ideal cell, the products recombine to form the reactants and thereby generate electrical power in an amount W_{FC} . The work output of the fuel cell is given by:

$$W_{\text{FC}} = -\Delta G|_{\text{H}_2 + 0.5\text{O}_2 \rightarrow \text{H}_2\text{O(l)}}. \quad (11)$$

The fuel cell operates isothermally; Q_{FC} is the amount of heat rejected to the surroundings:

$$Q_{\text{FC}} = -298 \text{ K} \times \Delta S|_{\text{H}_2 + 0.5\text{O}_2 \rightarrow \text{H}_2\text{O(l)}}. \quad (12)$$

Since the O₂ fed to the fuel cell is extracted from air, Eqs. (11) and (12) need to be corrected for the work expenditure for unmixing N₂ and O₂. The overall system efficiency of the closed-cycle is then calculated as:

$$\eta_{\text{overall}} = \frac{W_{\text{FC}}}{Q_{\text{solar}}}. \quad (13)$$

If we take into account, in addition to the work output of the cell, also the maximum available work (i.e. exergy) that can be extracted from essentially the sensible and latent heat of the products, the overall efficiency is then calculated as:

$$\eta_{\text{overall,max}} = \frac{W_{\text{FC}} + 298 \times Irr_{\text{quench}}}{Q_{\text{solar}}} \quad (14)$$

Eqs. (13) and (14) allows one to evaluate complex solar thermochemical processes by considering the maximum thermodynamic value of the chemical products as they recombined to form the reactants via an ideal reversible fuel cell. The calculation makes it possible to isolate the solar process and analyze it as a cyclic system: a heat engine that uses reactants and products as the *working fluid*, exchanges heat with the surroundings, and converts solar process heat into work. This analysis provides an especially useful basis for comparing the efficiencies of different solar processes.

5. RESULTS AND DISCUSSION

The baseline case is conducted at a constant total pressure of 1 atm. Reactants are fed at $T_1=298$ K and products are quenched to $T_3=298$ K. The reactor temperature T_2 is taken arbitrarily equal to 1900, 2100, 2300, and 2500 K. The mean flux concentration ratio is $\tilde{C}=5000$ suns (1 sun = 1 kW m^{-2}). A concentration ratio of 5000 is within the reach of large-scale solar collection facilities, provided that secondary concentrators, e.g. compound parabolic concentrators (CPC), are implemented (Welford and Winston, 1989). The mass flow-rate is 1 mol s^{-1} of $\text{Fe}_3\text{O}_4(\text{s})$ and $x \text{ moles s}^{-1}$ of air. Unless otherwise stated, the aforementioned baseline parameters are used. Table 1 shows the energy balance with and without quenching.

The solar absorption efficiency, $\eta_{\text{absorption}}$, decreases with temperature due to reradiation losses; it varies from 85% at 1900 K to 58% at 2500 K. A simple expression for the direct calculation of the change in absorption, as a function of the change in temperature ΔT is given by:

$$\begin{aligned} & (1 - \eta_{\text{absorption}@T}) / (1 - \eta_{\text{absorption}@T+\Delta T}) \\ & = [T / (T + \Delta T)]^4. \end{aligned} \quad (15)$$

The overall system efficiency with quenching, η_{overall} of Eq. (13), increases with temperature because the chemical conversion increases as well. Its value is 20% when complete conversion is assumed (Case 0), but is lower than 8% for all the remainder cases considered. The reason for such a low efficiency is clearly the loss of sensible heat by quenching, which amounts up to 80% of the solar energy input. There is a severe penalty for the large amount of energy needed to heat the reactants and air up to the reactor temperature and the subsequent quenching to avoid re-oxidation.

The irreversibilities in the reactor and during the quench reduce the efficiency from the Carnot value. They are produced by heat transfer across a finite temperature difference and by irreversible chemical reactions. Specifically, irreversibilities associated with heat transfer occur because the reactor at T_{reactor} re-radiates energy to the surroundings through the aperture; during the quench, heat transfer takes place between the hot products leaving the reactor and the cold sink. One can reduce the reactor irreversibility by increasing the concentration ratio (increasing \tilde{C} improves $\eta_{\text{absorption}}$ by reducing the portion of incoming radiation that is re-radiated to the sink).

One may be able to reduce the irreversibility of the quench. For example, if the kinetics or the reactor design permit the products to be cooled with a heat exchanger, one could pre-heat the reactants going into the solar receiver, or utilize the sensible and latent heat of the products to generate electric work via a heat engine. The maximum overall efficiency, $\eta_{\text{overall,max}}$ of Eq. (14), takes into account, in addition to the work output of the cell, also the maximum available work (i.e. exergy) that can be extracted from the products. These efficiencies, listed in the last row of Table 1, are remarkably higher, varying between 61% and 42% as the temperature varies between 1900 K and 2500 K.

The effect of doubling the solar concentration on the overall efficiency is shown in Table 2 for the baseline Case 0. The higher the concentration, the smaller the aperture, the less re-radiation losses, and consequently the higher the absorption and overall efficiencies. Concentration ratios of 10 000 and higher are theoretically achievable in solar central receiver plants, provided a CPC or other secondary concentrators are coupled to a narrow view angle of the heliostat field (Welford and Winston, 1989), but its technical and economical feasibility need still to be demonstrated.

5.1. Chemical by-products

The chemical products from each system component are either recycled or discarded. The gaseous products of the solar reactor after quenching are N_2 and O_2 , which are discharged to the atmosphere. The products of the water splitter are $\text{Fe}_3\text{O}_4(\text{s})$ and H_2 ; $\text{Fe}_3\text{O}_4(\text{s})$ is recycled to the solar reactor while H_2 is directed to the fuel cell. The product of the fuel cell is H_2O , which is recycled to the water splitter. An external source of air is

Table 2. Effect of doubling the solar concentration ratio on the efficiency of the cycle for Case 0

Case	0_1	0_2
Loading ratio	0	0
T_{reactor} (K)	2300	2300
Conversion ratio (%)	100%	100%
Concentration ratio	5000	10 000
Energy balance		
Q_{solar} (kW)	1148.6	932.2
Q_{rerad} (kW)	364.6	148.2
$Q_{\text{reactor,net}}$ (kW)	784.0	784.0
Q_{quench} (kW)		478.3
Q_{WS} (kW)		18.0
Q_{FC} (kW)		53.8
$\eta_{\text{absorption}}$ (%)	68.3%	84.1%
W_{FC} (kW)		233.9
η_{overall} (%)	20.4%	25.1%
$\eta_{\text{overall,max}}$ (%)	50.7%	62.5%

required for the carrier or quenching gas in the solar reactor, and as the oxidant of the fuel cell.

6. SOLAR CHEMICAL REACTOR CONCEPTS

The preceding analysis defines the constraints that the chemistry of the Fe_3O_4 -decomposition reaction places on the design for a solar thermal chemical reactor. From the thermodynamic and kinetic calculations, we determine the product composition and the optimum operating temperature for maximum chemical conversion ratio. The yield of FeO also depends on the quenching rate to avoid its re-oxidation, unless FeO is withdrawn from the reaction chamber in the absence of oxygen. From the second-law analysis, we conclude that a viable cycle efficiency can be obtained for a process that uses not only the work output of the fuel cell but also the maximum available work that can be extracted from the hot products exiting the solar reactor. It was shown that quenching the reaction products results in an unacceptable cycle efficiency. This implies that FeO(l) and O_2 must be in-situ separated (while they are hot in equilibrium inside the reactor) and subsequently the sensible and latent heat of the two product streams must be recovered.

Before proceeding with our design concepts, we summarize what we call the chemical boundary conditions for the reactor designer.

1. The reactor should operate at a temperature between 2100–2500 K. Thermal efficiencies are higher for the lower temperatures, but at the expense of moving more mass during the cycle because the chemical conversion ratio decreases with decreasing temperature.
2. The reactor should be open to the air. Little is gained in terms of thermal efficiency or conversion ratio by working under an inert atmosphere.
3. One must be able to control the residence time of the reactants so that one can maximize the daily yield of FeO. The kinetics of the decomposition reaction demonstrate that the reaction reaches a maximum rate near 40% completion.
4. The gas phase products must be in-situ separated from the condensed phase products to avoid the recombination reaction or to avoid producing an unacceptably high irreversibility by separating the products with a quench. FeO should be withdrawn from the reactor chamber in the absence of oxygen.

We present two reactor design concepts that address these boundary conditions. One is a

continuous gravity separation reactor to be used for a nearly vertical axis solar furnace. The second is a centrifugal reactor with semi-continuous separation to be used for a nearly horizontal axis solar furnace. Both reactor concepts feature three common characteristics: (1) they have a cavity-receiver configuration; (2) they use the reactants for lining the reactor inner walls; and (3) they offer the direct absorption of concentrated solar radiation. Cavity-receivers are insulated enclosures designed to effectively capture incident solar radiation entering through a small aperture. Because of multiple internal reflections, the cavity-receiver approaches a blackbody absorber. The shell of the cavity is made from conventional steel materials and lined with Fe_3O_4 particles, the same material as the reactants themselves. This aspect of the design eliminates the need for using expensive and difficult-to-fabricate ceramic insulating materials for ultra-high temperatures. It also offers excellent resistance to thermal shocks that are intrinsic in short start-ups solar applications. Direct-absorption is usually attributed to the absorption of concentrated solar energy by directly-irradiated fluids, particles, or surfaces, which serve simultaneously the functions of energy absorbers, heat transfer, and chemical reactants. Such a concept provides efficient radiation heat transfer directly to the site where the energy is needed, by-passing the limitations imposed by indirect heat transport via heat exchangers. The direct absorption concept has been experimentally demonstrated with gas-particle suspensions (Hunt *et al.*, 1986; Rightley *et al.*, 1992; Steinfeld *et al.*, 1994), with metallic wire mesh, perforated graphite disks, and ceramic honeycombs, grids, foams, cloths, and foils for absorbing and transferring heat to reactants or to air (Kappauf *et al.*, 1985; Böhmer and Chaza, 1991), with molten salt as the energy working medium (Klimas *et al.*, 1991), with fluidized beds (Rizzuti and Yue, 1983; Flamant *et al.*, 1980; Ingel *et al.*, 1992; Steinfeld *et al.*, 1993), with rotary-kiln and cyclone configurations for calcining limestone (Flamant *et al.*, 1988; Steinfeld *et al.*, 1992), with catalytic surfaces and particles in the methane-reforming and methane-cracking reaction (Levy *et al.*, 1992; Buck *et al.*, 1991; Steinfeld *et al.*, 1997), and with various solar photochemical applications (Blake, 1995).

(1) *The Gravity Separation Reactor Concept*—Fig. 3 illustrates the concept. A cavity-receiver is positioned vertically and concentrated solar radiation is impinging directly on the reactants from the top. It is initially filled with Fe_3O_4 which also

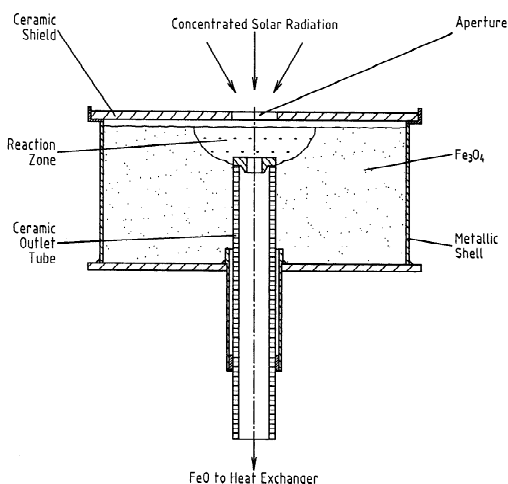


Fig. 3. Schematic of the 'gravity-separation' reactor concept for conducting the solar thermal reduction of Fe_3O_4 and in-situ separation of FeO and oxygen. It consists of a cavity-receiver, lined with Fe_3O_4 , that is positioned vertically. Concentrated solar radiation is impinging directly on the reactants from the top. As Fe_3O_4 melts and decomposes to FeO(l) , oxygen is liberated from the top while molten FeO is withdrawn from the bottom in the absence of air.

serves to line the reactor inner walls in such a way that a temperature gradient is created between the hot reaction zone and the cooler reactor walls. As Fe_3O_4 melts and decomposes to FeO(l) , oxygen is liberated from the top while molten FeO is withdrawn from the bottom in the absence of air.

(2) *The Centrifugal Reactor Concept with In-Situ Separation*—Fig. 4 illustrates the concept. A cavity receiver rotates around the horizontal axis. Reactants are continuously fed and products are continuously removed while effecting an in-situ

separation of condensed and gas phases by centrifugal force. These two stream of products are then used to preheat the incoming reactants. A batch of preheated reactants undergo thermal decomposition while hot O_2 and air are continuously removed out the back of the reactor. The gases pass through the next batch of Fe_3O_4 particles, thereby preheating them. After a specified residence time under solar irradiation, the reactor stops rotating. The FeO is allowed to drain from the reactor by mechanically removing a plug made from dense ZrO_2 . The sensible energy in the FeO would be also used to preheat the incoming reactants, however the details of this step are not shown. A new batch of Fe_3O_4 would be supplied and the process repeated.

These two reactor concepts satisfy the chemical boundary conditions dictated by the chemistry of the decomposition reaction. They each allow for a way to obtain FeO from the decomposition of Fe_3O_4 while minimizing the irreversibility of the separation step. The reactor can be designed to work in air at temperatures near 2500 K. The operator of the reactor has complete control of the residence time.

7. CLOSING REMARKS

The purpose of this paper was to demonstrate a methodology by which one can begin to proceed with the development of a solar thermal chemical reactor that some day may be economically viable for producing fuels from sunlight. The method demonstrates that the chemistry of the reaction to be effected in the reactor places important initial constraints on the reactor design. The design

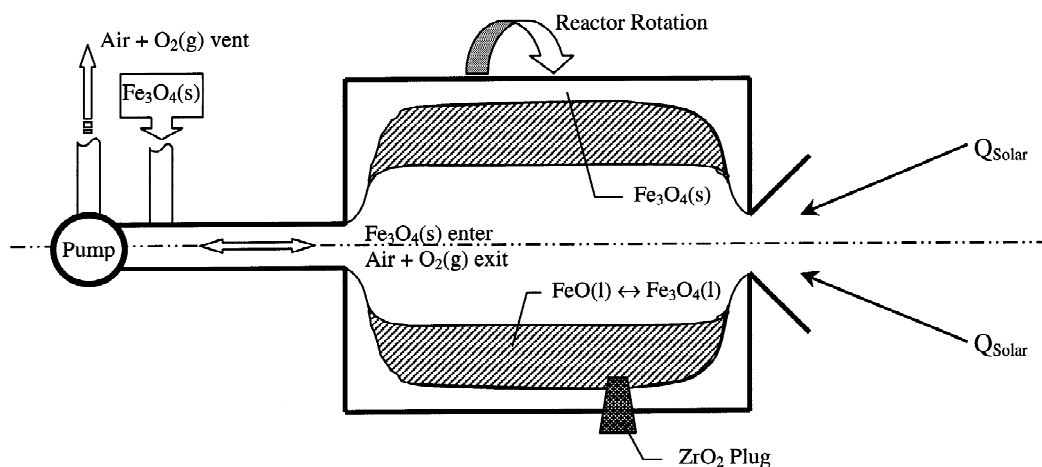


Fig. 4. Schematic of the 'centrifugal' reactor concept for conducting the solar thermal reduction of Fe_3O_4 and in-situ separation of FeO and oxygen. It consists of a cavity-receiver that rotates around the horizontal axis. Reactants are continuously fed and products are continuously removed while effecting an in-situ separation of condensed and gas phases by centrifugal force.

work, though is far from complete. At this juncture a number of fundamental design questions remain that must be systematically answered by experimental and analytical work. The answers in turn will likely force several iterations on the initial reactor concepts.

For example, the reactor ultimately must be economically and technically feasible. In this regard one must demonstrate the feasibility of the in-situ separation. More physiochemical data must be obtained for Fe_3O_4 and FeO. Our current understanding of the thermodynamics of the FeO and Fe_3O_4 liquid system prevents us from confidently estimating thermal efficiencies and mass flow-rates. We need a better understanding of the kinetics of the decomposition reaction if we are to accurately predict daily FeO yields. One must demonstrate the conditions for which the reactor will function with a high solar absorption efficiency and low convection losses using conventional materials. The irreversibility of the pre-heating steps must be minimized through careful heat transfer design. Design features must enable the reactor to be scaled up to large solar power inputs and to remain intact for thousands of hours of operation even while experiencing severe thermal shocks.

Our experience suggests that these important remaining questions, design problems, and demonstrations are most comfortably approached if one has a clear picture of how the reactor in the end will efficiently deal with the chemistry of the reaction. Much of the work in developing a new technology is necessarily done in a shroud of unknowns and uncertainties. Using the Fe_3O_4 -decomposition as a case study, we have presented the initial steps necessary for the design of a solar chemical reactor.

NOMENCLATURE

\bar{C}	Mean flux solar concentration
ΔG	Gibbs free energy change (kW)
ΔH	Enthalpy change (kW)
ΔS	Entropy change (kW)
I	Normal beam insolation (kW m^{-2})
Irr_{quench}	Irreversibility associated with the quenching (kW K^{-1})
Q_{FC}	Heat rejected to the surroundings by the fuel cell (kW)
Q_{quench}	Heat rejected to the surroundings by the quenching process (kW).
$Q_{\text{reactor,net}}$	Net power absorbed by the solar reactor (kW)
Q_{rerad}	Power re-radiated through the reactor aperture (kW)
Q_{solar}	Total solar power coming from the concentrator (kW)

Q_{ws}	Heat rejected to the surroundings by the water-splitter (kW)
T_{reactor}	Nominal cavity-receiver temperature (K)
W_{FC}	Work output by the fuel cell (kW)
$\alpha_{\text{eff}}, \epsilon_{\text{eff}}$	Effective absorptance and emittance of the solar cavity-receiver
$\eta_{\text{absorption}}$	Solar energy absorption efficiency
η_{overall}	Overall system efficiency
$\eta_{\text{overall,max}}$	Overall efficiency of an ideal solar-Carnot system
σ	Stefan-Boltzmann constant ($5.6705 \times 10^{-8} \text{ W m}^{-2} \text{ K}^{-4}$)

Acknowledgements—We gratefully acknowledge the financial support of BFE-Swiss Federal Office of Energy. We thank D. Wuillemin and A. Meier for their help in the conceptual design of solar reactors, and M. Sturzenegger and E. Steiner for their critical review of the manuscript.

REFERENCES

- Blake D. (1995) *Bibliography of Work on the Photocatalytic Removal of Hazardous Compounds from Water and Air*, National Renewable Energy Laboratory, NREL/TP-473-20300, Golden, CO, USA.
- Böhmer M. and Chaza C. (1991) The ceramic foil volumetric receiver. *Solar Energy Mater.* **24**, 182–191.
- Buck R., Muir J. F., Hogan R. E. and Skocypec R. D. (1991) Carbon dioxide reforming of methane in a solar volumetric receiver/reactor: the Caesar project. *Solar Energy Mater.* **24**, 449–463.
- Ehrensberger K., Frei A., Kuhn P., Oswald H. R. and Hug P. (1995) Comparative experimental investigations of the water-splitting reaction with iron oxide Fe_{1-y}O and iron manganese oxides $(\text{Fe}_x\text{Mn}_{1-x})_{1-y}\text{O}$. *Solid State Ionics* **78**, 151–160.
- Ehrensberger K., Palumbo R., Larson C. and Steinfeld A. (1997) Production of carbon from CO_2 with iron oxides and high-temperature solar energy. *Ind. Eng. Chem. Res.* **36**, 645–648.
- Flamant G., Hernandez D., Bonet C. and Traverse J. (1980) Experimental aspects of the thermochemical conversion of solar energy: decarbonation of CaCO_3 . *Solar Energy* **24**, 385–395.
- Flamant G., Gauthier D., Boudhari C. and Flitris Y. (1988) A 50 kW fluidized bed high temperature solar receiver: heat transfer analysis. *Solar Energy Eng.* **110**, 313–320.
- Fletcher E. A. and Moen R. L. (1977) Hydrogen and oxygen from water. *Science* **197**, 1050–1056.
- Hunt A.J., Ayer J., Hull P., Miller F., Noring J. E. and Worth D. (1986) *Solar Radiant Heating of Gas-Particle Mixtures*, Lawrence Berkeley Laboratory LBL-22743, University of California, Berkeley, CA 94720, USA.
- Ingel G., Levy M. and Gordon J. (1992) Oil-shale gasification by concentrated sunlight: an open-loop solar chemical heat pipe. *Energy – Int. J.* **17**, 1189–1197.
- JANAF Thermochemical Tables* (1985) National Bureau of Standards, 3rd ed., Washington, D.C., USA.
- Kappauf T., Murray J. P., Palumbo R. D., Diver R. B. and Fletcher E. A. (1985) Hydrogen and sulfur from hydrogen sulfide – IV. Quenching the effluent from a solar furnace. *Energy – Int. J.* **10**, 1119–1137.
- Klimas P. C., Diver R. B. and Chavez J. (1991) United States Department of Energy solar receiver development. *Solar Energy Materials* **24**, 136–150.
- Kuhn P., Ehrensberger K., Steiner E. and Steinfeld A. (1995) An Overview on PSI's high-temperature solar chemistry research. In *Solar Engineering 1995 - Proceedings ASME International Solar Energy Conference*, pp. 375–380, Hawaii, USA.

- De Laquil P. (1994) Status of solar tower development. In *Proceedings 7th Int. Symp. Solar Thermal Concentrating Technologies*, pp. 59–71, Moscow, Russia.
- Lede J. and Pharabod F. (1997) Chimie solaire dans le Monde et en France. *Entropie* **204**, 47–55.
- Levy M., Rubin R., Rosin H. and Levitan R. (1992) Methane reforming by direct solar irradiation of the catalyst. *Energy – Int. J.* **17**, 749–750.
- Nakamura T. (1977) Hydrogen production from water utilizing solar heat at high temperatures. *Solar Energy* **19**, 467–475.
- Nüesch P. (1996) *Diplomarbeit*, University of Zurich, Switzerland
- Reynolds W.C. (1986) *The Element Potential Method for Chemical Equilibrium Analysis*, Stanford University, USA.
- Rightley M. J., Matthews L. and Mulholland G. (1992) Experimental characterization of the heat transfer in a free-falling-particle receiver. *Solar Energy* **48**, 363–374.
- Rizzuti L. and Yue P. (1983) The measurement of light transmission through an irradiated fluidized bed. *Chem. Eng. Sci.* **38**, 1241–1249.
- Sibieude F., Ducarroir M., Tofighi A. and Ambriz J. (1982) High temperature experiments with a solar furnace: the decomposition of Fe_3O_4 , Mn_3O_4 , CdO . *Int. J. Hydrogen Energy* **7**, 79–88.
- Steinfeld A., Imhof A. and Mischler D. (1992) Experimental investigation of an atmospheric-open cyclone solar reactor for solid–gas thermochemical reactions. *J. Solar Energy Eng.* **114**, 171–174.
- Steinfeld A., Kuhn P. and Karni J. (1993) High-temperature solar thermochemistry: production of iron and synthesis gas by Fe_3O_4 – reduction with methane. *Energy – Int. J.* **18**, 239–249.
- Steinfeld A., Brack M., Ganz J., Haueter P., Imhof A., Meier A., Mischler D., Nater E., Seitz T., Schwarz A. and Wuillemin D. (1994) Particle-cloud reactor development for high-temperature solar chemistry. In *Proceedings 7th Int. Symp. Solar Thermal Concentrating Technologies*, Vol. 4, pp. 888–895, Moscow, Russia.
- Steinfeld A., Larson C., Palumbo R. and Foley M. (1996) Thermodynamic analysis of the co-production of zinc and synthesis gas using solar process heat. *Energy – Int. J.* **21**, 205–222.
- Steinfeld A., Kirillov V., Kuvshinov G., Mogilnykh Y. and Reller A. (1997) Production of filamentous carbon and hydrogen by solarthermal catalytic cracking of methane. *Chem. Eng. Sci.* **52**, 3599–3603.
- Steiner E. (1997) *Internal Report*, Paul Scherrer Institute, CH-5232 Villigen, Switzerland.
- Tamaura Y., Steinfeld A., Kuhn P. and Ehrensberger K. (1995) Production of solar hydrogen by a novel, two-step, water-splitting thermochemical cycle. *Energy – Int. J.* **20**, 325–330.
- Tofighi A. (1982) *Ph.D. Thesis*, L’Institut National Polytechnique de Toulouse, Toulouse, France.
- Tofighi A. and Sibieude F. (1980) Note on the condensation of the vapor phase above a melt of iron oxide in a solar parabolic concentrator. *Int. J. Hydrogen Energy* **5**, 375–381.
- Tofighi A. and Sibieude F. (1984) Dissociation of magnetite in a solar furnace for hydrogen production. Tentative production evaluation of a 1000 kW concentrator from small scale (2 kW) experimental results. *Int. J. Hydrogen Energy* **9**, 293–296.
- Welford W.T. and Winston R. (1989) *High Collection Nonimaging Optics*, Academic Press, San Diego, USA.